ORIGINAL PAPER

CrossMark

Dynamic effects on cutting forces with highly positive versus highly negative cutting edge geometries

A. Agic[1,2] · M. Eynian[2] · J.-E. Ståhl[3] · T. Beno[2]

Abstract

Understanding the influence of the cutting edge geometry on the development of cutting forces during the milling process is of high importance in order to predict the mechanical loads on the cutting edge as well as the dynamic behavior on the milling tool. The work conducted in this study involves the force development over the entire engagement of a flute in milling, from peak force during the entry phase until the exit phase. The results show a significant difference in the behavior of the cutting process for a highly positive versus a highly negative cutting edge geometry. The negative edge geometry gives rise to larger force magnitudes and very similar developments of the tangential and radial cutting force. The positive cutting edge geometry produces considerably different developments of the tangential and radial cutting force. In case of positive cutting edge geometry, the radial cutting force increases while the uncut chip thickness decreases directly after the entry phase; reaching the peak value after a certain delay. The radial force fluctuation is significantly higher for the positive cutting edge geometry. The understanding of such behavior is important for modelling of the milling process, the design of the cutting edge and the interactive design of digital applications for the selection of the cutting parameters.

Keywords Milling · Cutting force · Cutting edge geometry · Frequency spectrum · RMS

1 Introduction

The design of the cutting edge is commonly defined by its geometrical parameters such as rake angle, edge hone, width and angle of the protection chamfer. All these parameters have tremendous influence on the milling process and are often optimized for certain milling applications, workpiece materials and cutting parameters. Positive cutting edge geometries are often used in milling applications of workpiece materials that have a strong adhesion and/or smearing behavior or for materials prone to show deformation hardening while cutting geometries with negative protection chamfers are used in hard and brittle workpiece materials, particularly in roughing applications.

Cutting forces in milling have been investigated in numerous research studies [1–4]. The forces are dependent on cutting parameters and cutting force coefficients. The cutting force coefficients are in turn dependent on both: the workpiece material and the geometry of the cutting edge. In general, the relationship between the cutting forces and the uncut chip thickness is established from experimental data, i.e. mechanistic force modelling [5–7]. Both linear and nonlinear [8] models can be used depending on the curve fitting technique applied. These models include the variation of the chip thickness and the cutting resistance related to the workpiece material but do not include for any dynamic effects related to the chip segmentation or the transient vibrations caused by the entry and exit phases. Influence from the entry phase has a significant effect on the tool life and has been shown in [9–11] while the exit phase and its influence on the tool life has been investigated in [12, 13]. Further, influence from the entry phase on vibrations is examined in [14] where it is shown that the entry phase has a great impact on magnitude and frequency band of the system excitation. The cutting force model proposed in [15] includes the dynamic effects,
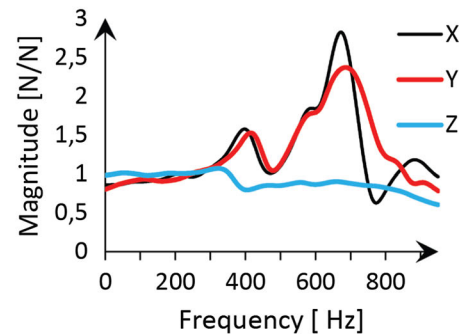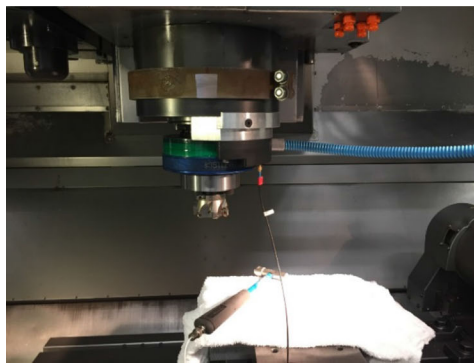
✉ A. Agic
  adnan.agic@secotools.com

1 Seco Tools, Fagersta, Sweden

2 Department of Engineering Science, University West, Trollhättan, Sweden

3 Production and Materials Engineering, Lund University, Lund, Sweden

Fig. 1 The rotating
dynamometer and its frequency
response function

2 Methodology

Two significantly different cutting edge geometries are used in the experimental tests. Highly positive cutting edge geometry has a large rake angle, non-protection chamfer and rather small edge hone. Highly negative cutting edge geometry has very low rake angle, large and negative protection chamfer and moderate edge hone.

The cutting forces are measured for both cutting edge geometries at various feeds and spindle speeds. The axial depth of cut was 8 mm while the width of cut was 31.5 mm. The diameter of the milling cutter used was 63 mm.

The cutting forces are measured by the use of a piezo dynamic force sensor connected to a data acquisition system. The obtained signals are then analyzed as a function of the uncut chip thickness during the engagement of a milling flute in both time and frequency domain using an algorithm developed.

which showed enhanced agreement with the measured cutting forces than the rigid model. The variation in cutting forces as a function of the instantaneous chip thickness is the core of the stability concept, explained in [16–18]. The actual cutting force is also affected by the dynamic properties of the machine tool-workpiece system, workpiece material, cutting parameters and cutting edge geometry.

Consequently, the actual peak value of the cutting force and its variation over the entire engagement of a milling flute depends on the several parameters that often interact simultaneously in a milling operation.

The work presented herein explores the influence of a highly negative and highly positive cutting edge geometries on the dynamic force development over the engagement, including the entry, full engagement and exit phases. It explains the main difference in the force build up process between these geometries which is important for deeper understanding of the stress state in the cutting edge and cutting dynamics.

2.1 Measurement methods

Cutting forces were measured with a rotating piezo dynamometer, shown in Fig. 1. The measurements were carried out in a 3 axis milling machine equipped with a BT50 tool-spindle interface. The dynamometer measures tangential, radial and axial components of the cutting force in a rotating coordinate system. The sampling frequency used for the cutting force measurements was 5 kHz. Prior to the measurements, the frequency range of the dynamometer in the given set up has been analyzed. The frequency response function of the dynamometer is obtained by an impact hammer excitation of the dynamometer and simultaneous measurement of the input and output forces. The hammer excitation is done by an impact hammer. The relationship between the output and input force as a function of the frequency is obtained. The frequency response functions, FRF for x, y and z directions, are shown in Fig. 1. It can be realized from the obtained FRF that the linearity of the measurement system is satisfactory up to 300 Hz. Based on that, a low pass filter of Butterworth type with the cut off frequency of 300 Hz has been used to remove the effects of the natural modes and measurement distortions from the force signals.

The low pass filter removes also the contribution of the frequency components higher than the cut off frequency 300 Hz which have a certain effect on the peak force magnitudes. This effect has been neglected in this study.

2.2 Cutting edge geometries and workpiece

The milling cutter used in the experiments is a square shoulder milling cutter, type R220.69-0063-12-6A. The experiments are conducted by only one insert mounted in the cutter, i.e. the effective number of teeth is 1. Two different cutting edge geometries have been evaluated in the performed experiments. These cutting geometries are commonly used in different milling applications and workpiece materials in the machining industry. The helix angle and positioning in the pocket are identical for both cutting geometries. Four parameters that are dependent on the cutting edge geometry

Table 1 Cutting edge geometries, normalized values

Cutting edge geometry	γ	b_n	γ_n	ER, edge hone
Negative	0	1	1	1
Positive	1	–	–	0.4
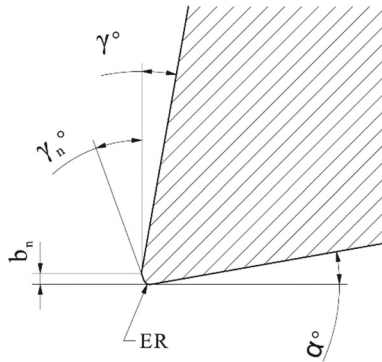
Fig. 2 Cutting edge geometry

Table 2 Cutting parameters used in the experiments

Cutting speed (m/min)	Feed (mm/tooth)		
140	0.1	0.15	0.2
180	0.1	0.15	0.2
220	0.1	0.15	0.2

are: rake angle, width of protection chamfer, angle of protection chamfer and edge hone. The substrate and coating are identical for both cutting geometries. The complete description of the cutting geometries with the normalized values is given in Table 1 and Fig. 2. The values shown in Table 1 are computed from the effective values when the insert is mounted in the pocket seat.

The work piece material is steel, 42 CrMo4 in the shape of a bar with length of 300 mm and quadratic cross section of 100 mm. Cutting parameters are shown in Table 2. The cutting force measurements have been carried out for each cutting edge geometry and cutting condition which in total produced 18 measurements.

2.3 Evaluation of cutting force

The development of the tangential and radial cutting force is shown as a function of time for both cutting edge geometries and all cutting conditions used. The significant difference on the development of the radial forces is clearly shown in the obtained graphs.

The force spectrums are computed by an algorithm utilizing the following theoretical approach: The discrete Fourier transform, DFT is applied on the tangential and radial cutting forces. As the cutting forces are assumed to be periodic, the root mean square, RMS scaled spectrums are established [19]. The RMS spectrums give the RMS value for each frequency component in the spectrum. A flattop window is utilized to counteract the leakage prior to the execution of the DFT. The loss of energy in the signal due to windowing is then compensated with spectrum scaling to ensure the accuracy of the RMS value for the frequency components in the cutting force spectrums. The following expression is applied in the computation of the force spectrums,

$$S_{xx} = \frac{1}{M} \sum_{m=1}^{M} 2 \left| \frac{DFT\{x(n) \cdot w(n)\}}{C_A \cdot N} \right|^2 \tag{1}$$

The window compensation is computed according to the following equation,

$$C_A = \frac{\sum_{n=0}^{N-1} w(n)}{N} \tag{2}$$

As there might be certain variations of the force magnitudes over the entire force signal, the averaging is employed using the M number of the spectrums with N block size. Afterwards the DFT results are averaged for every frequency component in the spectrum. In the computation of the spectrum the overlap of 50% of the block size N is used. Taking the square root of S_{xx} in the Eq. (1) generates the peaks in the spectrum that correspond to RMS values.

$$RMS_k = \sqrt{S_{xx}} \tag{3}$$

The obtained spectrums allow the comparison of RMS amplitudes between cutting edge geometries and different cutting conditions.

3 Results and analysis

3.1 Time domain

The tangential forces for the positive and negative cutting edge geometries are shown in Fig. 3. The development of the tangential cutting forces is almost identical for both cutting edge geometries. It is noteworthy that the variation of the tangential cutting forces exhibits the same shape. The main difference is on the magnitudes, which is dependent on the cutting parameters. The peak value is reached during the entry phase. As the uncut chip thickness decreases the tangential cutting force decreases. Despite the low-pass filter (300 Hz), a considerable fluctuation of the forces can be found. This is clearly observable at the entry phase which
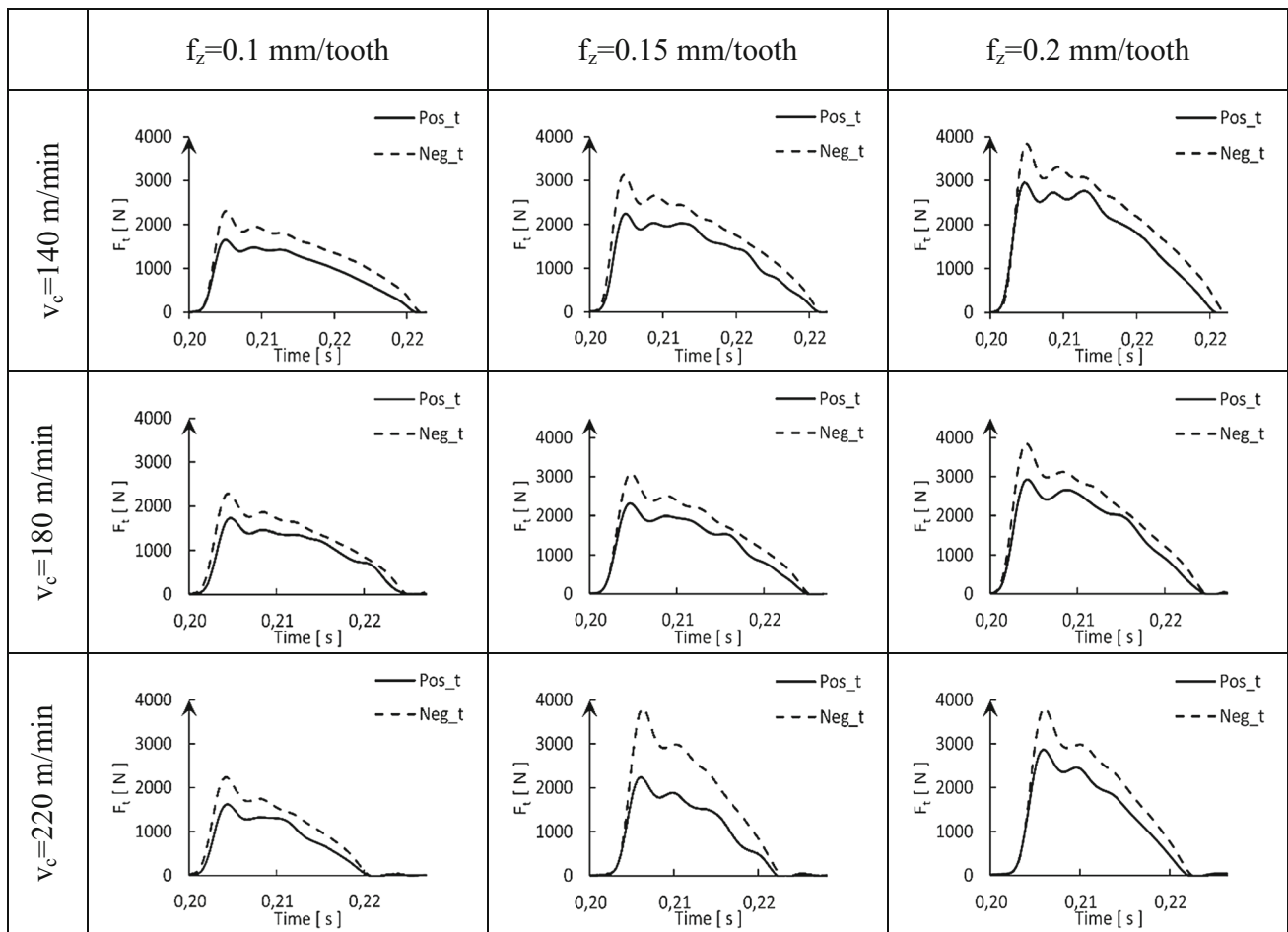
Fig. 3 Tangential cutting forces

gives rise to impact load and subsequent fluctuation of the tangential forces for both cutting edge geometries.

However, the radial forces show a significant difference between the cutting edge geometries: both the magnitudes as well as the force development during engagement exhibit a different behavior. The negative cutting edge geometry produces a similar development of the radial and tangential cutting force, *i.e.* the peak value during entry phase followed by a transient behavior of the cutting force. On the contrary, a highly positive cutting edge geometry does not reach the peak radial forces during the entry phase, which is shown in Fig. 4. In essence, the radial cutting force increases while the chip thickness decreases during the first half of the engagement phase. The peak of the radial force is reached after a significant delay in relation to the entry phase for almost all cutting parameters investigated. Moreover, the radial forces are accompanied by a significant fluctuation during the entire engagement. This behavior is reinforced by the increase of the feed per tooth and cutting speed which is observable from Fig. 4.

The specific cutting forces in the radial direction, calculated as a ratio of the measured cutting forces and uncut chip load area, are shown in Fig. 5. The higher variation of the specific cutting force for the positive cutting edge geometry, computed with this approach, is illustrated in the right image of Fig. 5.

Even if the negative cutting edge geometry produces higher forces, the relation between the radial and tangential forces results in a more favorable state of the stress in this cutting edge, *i.e.* it is beneficial to reduce the tensile stresses in the cutting edges as these stresses cause chipping and sudden breakages.

A FE simulation has been carried out with the negative and positive cutting edge geometries and for one of the cutting conditions used $f_z = 0.2$ mm/tooth and $v_c = 140$ m/min, in order to illustrate this behavior. The workpiece material was AISI 4140. The set-up of the milling simulation is shown in Fig. 6.

Even if the entry conditions are not identical to the real machining case due to the predefined chip load section on the workpiece, the comparison between the cutting edge
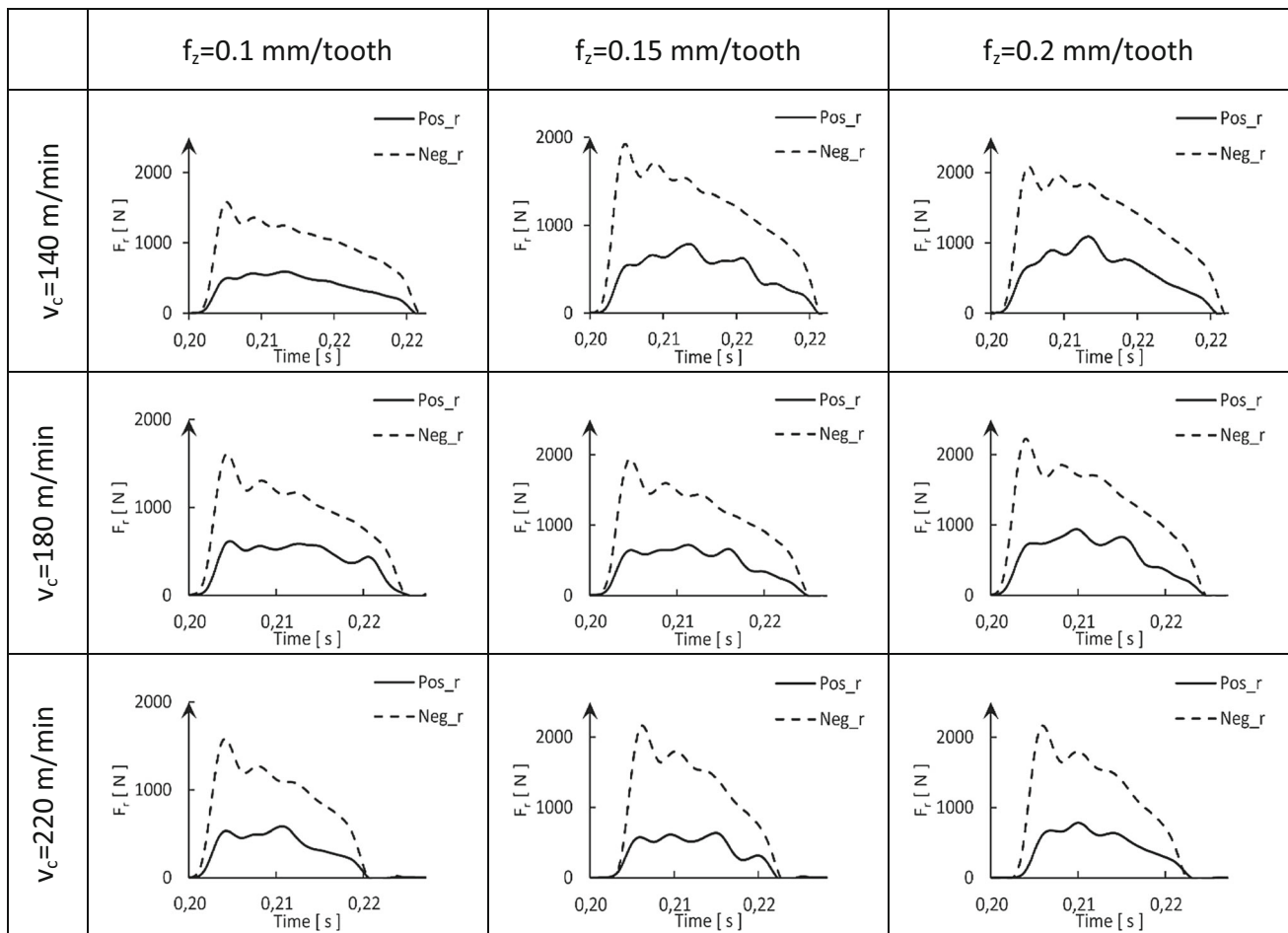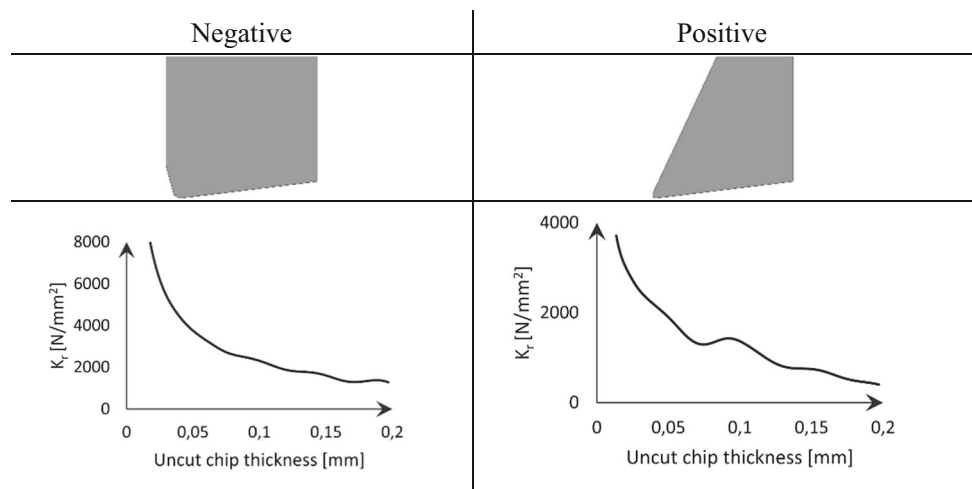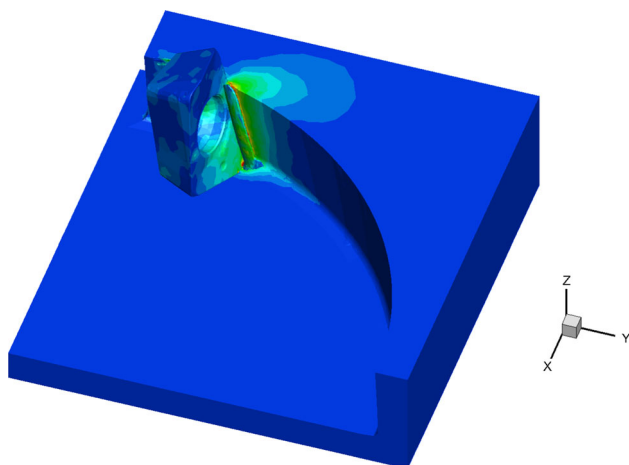
Fig. 4 Radial cutting forces

Fig. 5 Specific cutting force in radial direction: $f_z = 0.2$ mm/tooth, $v_c = 140$ m/min

geometries at the position shown in Fig. 6 gives a good indication about the difference of the stress states for the cutting edge geometries used. The maximum principle stresses at the insert position according to the Fig. 6 are displayed for both cutting edge geometries in Fig. 7.

It is observable from Fig. 7 that the tensile stresses are higher for the positive cutting edge geometry. These stresses are localized in the vicinity of the tool tip but also at a certain distance from the tool-chip interface. Although the positive cutting edge geometry has smaller wedge angle, *i.e.* smaller

Fig. 6 Milling simulation; $f_z = 0.2$ mm/tooth, $v_c = 140$ m/min

critical area of the cutting edge which combined with the magnitude of the cutting force can give rise to higher stresses in the cutting edge, the ratio between the radial and tangential forces itself can also contribute to the increase of the tensile stresses on the rake surface. Similar effects of the force distribution on the stress state in the cutting edge in case of intermittent turning and entry phase have been reported in [20].

It is evident from Fig. 4 that the radial force for the positive cutting edge geometry increases while the uncut chip thickness reduces after the entry phase until the instant the peak force is reached. A significant fluctuation of the radial force is found during this period for the positive cutting edge geometry while the force fluctuation for the negative cutting edge geometry is mostly related to the entry phase and

transient vibrations. Such a different cutting behavior can be caused by dynamics during cutting action or a real variation of the cutting resistance in the workpiece material.

An explanation of the presented behavior can be the difference in process damping for the cutting edge geometries used. Process damping is explained in [21–23]. The main parameters that affect process damping are flank surface of the cutting edge, i.e. relief angle, edge hone and vibration frequency. The increase of the edge hone as well as the reduction of the relief angle have diminishing effect on the tool vibrations. The influence of the protection chamfer on vibrations is incorporated through cutting force coefficients while its role on process damping has not been investigated. The influence of the chamfered tools on the tool life has been investigated in [24], while the difference between the honed and chamfered cutting edges has been examined in [25]. Analytical modelling of the cutting mechanics involving the protection chamfer has been done in [26]. These research works highlight the importance of the chamfer for the average cutting forces but do not consider any fluctuation of the cutting force during a milling engagement.

The results of this study strongly indicate that the interaction between the rake angle and protection chamfer has a large impact not only on the peak magnitudes but also force development and its variation during cutting process. The fluctuation of the cutting force during an engagement affects both the stresses and the fatigue life of the cutting edge. That is very important, especially for a highly positive cutting edge geometry which is sensitive to chipping. It is of high interest to design the cutting edges to reduce the forces and vibrations in the cutting process and at the same time ensure the strength of the cutting edge and reliability of the tool.
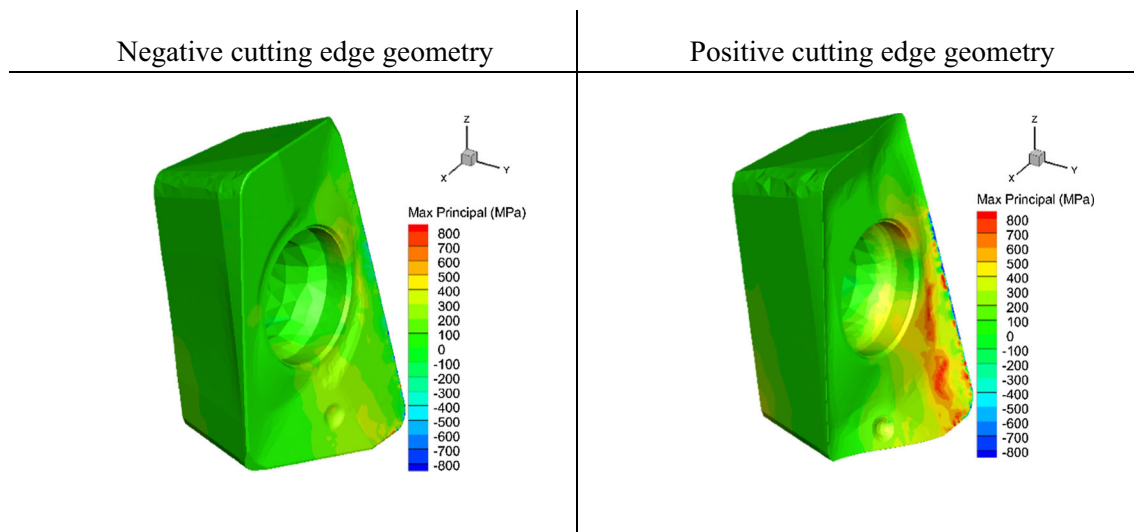
Fig. 7 Maximum principle stresses in the cutting edges
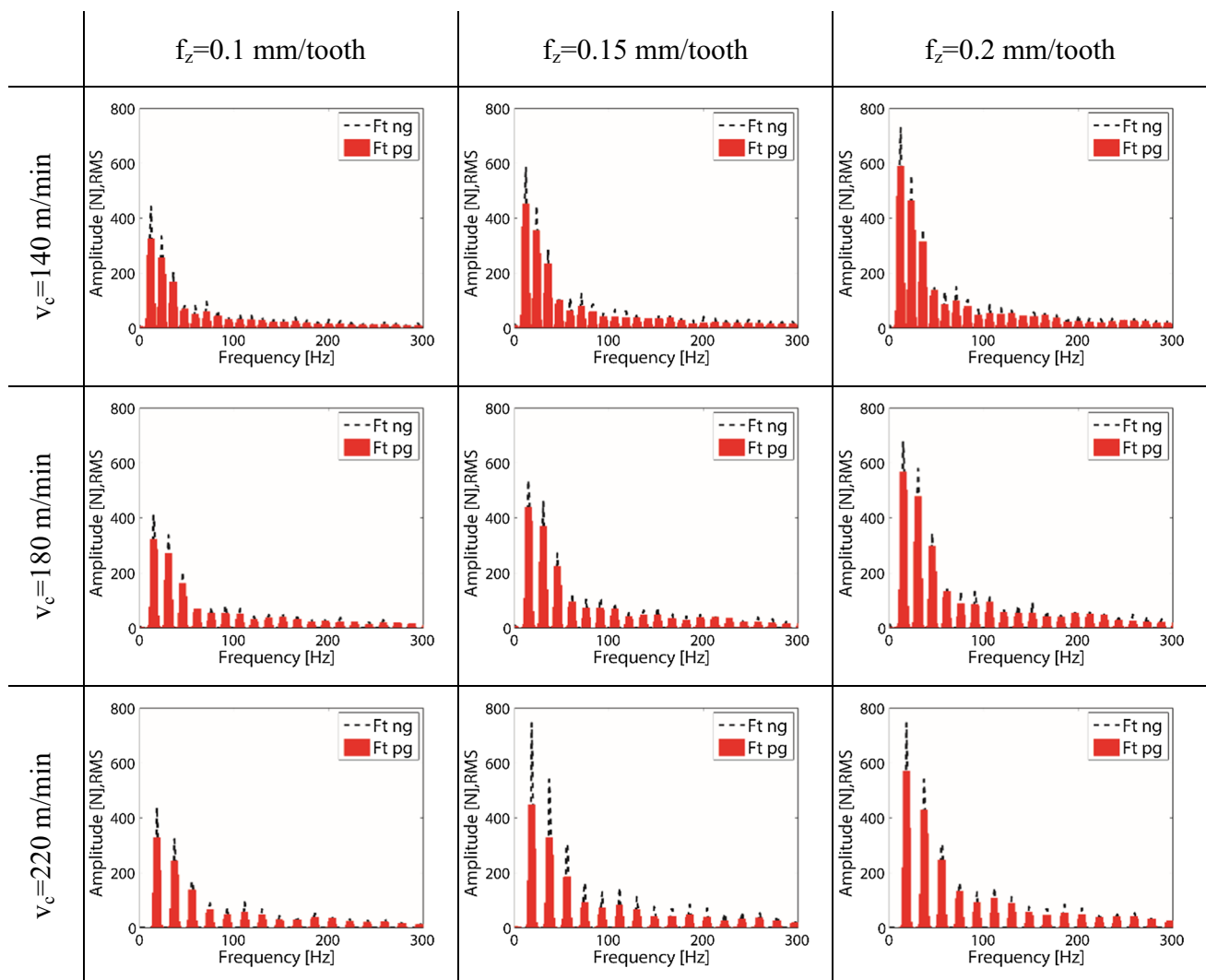
Fig. 8 Tangential force spectra for negative and positive cutting edge geometry

3.2 Frequency domain

The RMS spectrums for the tangential cutting forces on both cutting edge geometries are shown in Fig. 8. The significant difference of the RMS values is evident for the first three harmonics. This difference decreases at higher harmonics. Increasing the feed per tooth causes greater RMS values while the increase of the cutting speed can show both an increasing as well as a diminishing effect on the RMS values.

However, the RMS spectrums of the radial cutting forces give a significant difference for the entire frequency range. This is the main difference between a highly negative and a highly positive cutting edge geometry. Since the difference is apparent at the higher harmonics, this behavior can be addressed to the smooth entry phase and low impact force in the radial direction when using highly positive cutting edge

geometry. An increasing trend on the fourth, fifth and sixth harmonics is shown for the negative cutting edge geometry, while the positive geometry does not show a clear trend for these harmonics (Fig. 9).

Since the forces are filtered by the low-pass filter of 300 Hz, the resonance effects of the spindle—milling tool are removed. It is also notable that the force spectrums do not contain any specific harmonic generating sudden amplitude increase in the analyzed frequency range.

4 Conclusions

The tangential force exhibits identical behavior regardless of the cutting edge geometry. However, the radial force is importantly different in comparison to the tangential force: both the entry phase and the fluctuation of the radial force
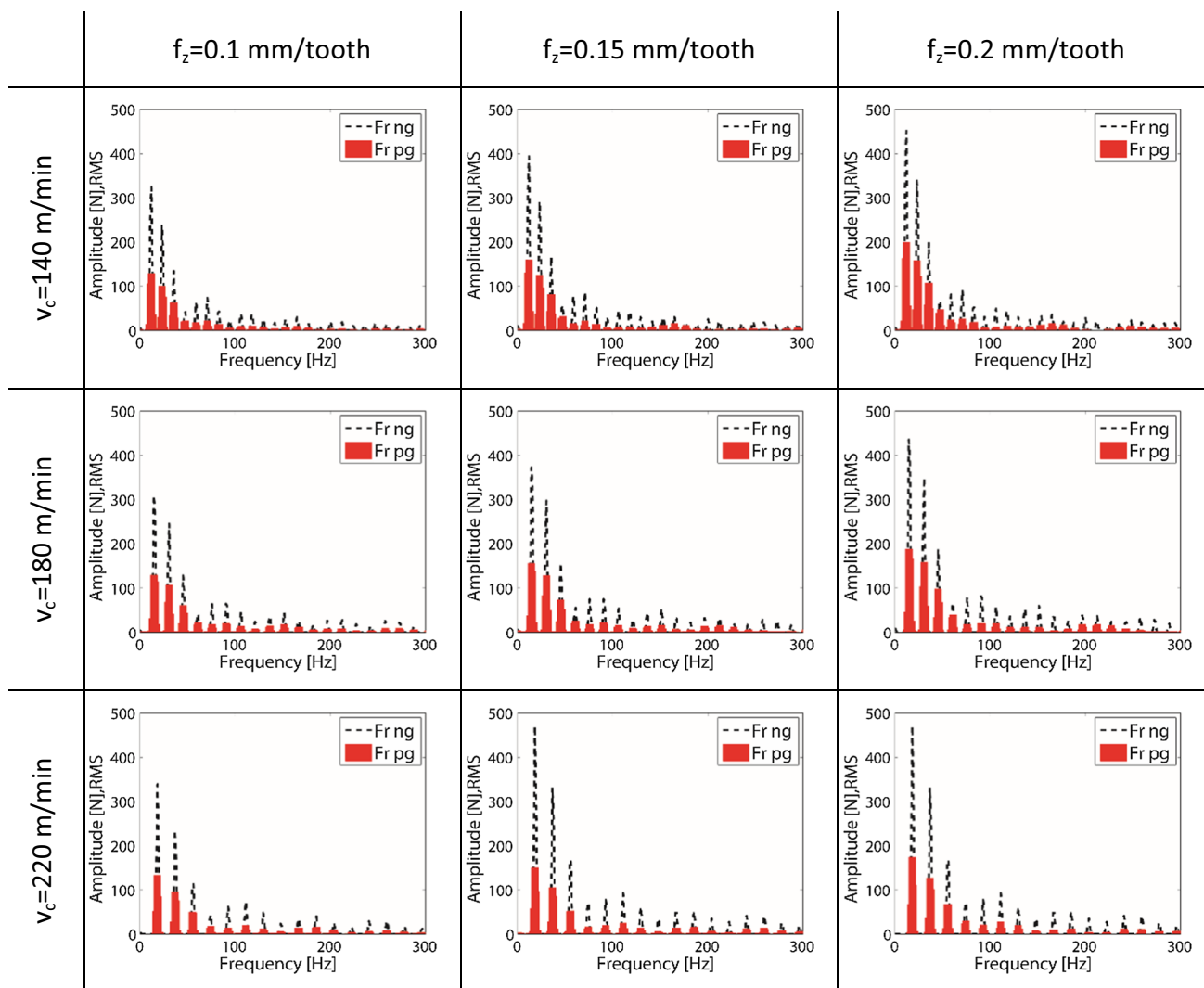
Fig. 9 Radial force spectra for negative and positive cutting edge geometry

are strongly dependent on the cutting edge geometry. While the peak of the tangential force is found during the entry phase for both cutting edge geometries, the peak of the radial force for the highly positive cutting edge geometry is reached after a significant delay in relation to the entry phase. This behavior may be due to the high rake angle, the absence of the protection chamfer and smaller edge hone. Nevertheless, such a force development is unfavorable for the stress state in the cutting edge. Large tangential and low radial forces tend to give rise to high tensile stresses in the cutting edge which causes chipping and sudden breakage.

The negative cutting edge geometry produces higher magnitudes for all frequency components in the force spectrums. The fluctuation of the radial forces in the time domain cannot be addressed to a specific frequency range. This fluctuation seems to be composed of a large number of harmonics. The negative cutting edge geometry gives rise to the fluctuation

caused by the entry phase while the increased fluctuation of the radial forces for the positive cutting edge geometry originates from the cutting process itself. The negative cutting edge geometry has a larger edge hone in comparison to the positive cutting edge geometry which can result in higher process damping. However, as the fluctuation of the radial cutting forces is not characterized with a specific frequency range, it is rather unclear if this behavior is caused by process damping or variation of the cutting resistance in the workpiece. It is notable that the rake angle and protection chamfer have great impact on the dynamic cutting force in milling. Whether their influence on the machining dynamics is completely covered by the cutting force coefficients, or that they have an important effect on the process damping is worthwhile to investigate in greater detail. The methods presented in this research study, *i.e.* RMS of the cutting forces and the calculation of the stress level in the cutting edge can

be utilized in the interactive design of digital applications to optimize the cutting edge geometry and the cutting parameters in industrial applications.

References

1. Koenigsberger, F., Sabberwal, A.J.P.: An investigation into the cutting force pulsations during milling operations. Int. J. Mach. Tool Des. Res. **1**(1–2), 15–33 (1961)
2. Budak, E.: Analytical models for high performance milling. Part I: cutting forces, structural deformations and tolerance integrity. Int. J. Mach. Tools Manuf **46**(12–13), 1478–1488 (2006)
3. Altintas, Y.: Manufacturing Automation: Metal Cutting Mechanics, Machine Tool Vibrations, and CNC Design. Cambridge University Press, Cambridge (2012)
4. Altintas, Y., Spence, A., Tlusty, J.: End milling force algorithms for CAD systems. CIRP Ann. **40**(1), 31–34 (1991)
5. Budak, E., Altintaş, Y., Armarego, E.J.A.: Prediction of milling force coefficients from orthogonal cutting data. J. Manuf. Sci. Eng. **118**(2), 216–224 (1996)
6. Gonzalo, O., Beristain, J., Jauregi, H., Sanz, C.: A method for the identification of the specific force coefficients for mechanistic milling simulation. Int. J. Mach. Tools Manuf. **50**(9), 765–774 (2010)
7. Gradišek, J., Kalveram, M., Weinert, K.: Mechanistic identification of specific force coefficients for a general end mill. Int. J. Mach. Tools Manuf. **44**(4), 401–414 (2004)
8. Kienzle, O.: Die Bestimmung von Kräften und Leistungen an spanenden Werkzeugen und Werkzeugmaschinen. VDI-Z **94**(11–12), 299–305 (1952)
9. Kronenberg, M.: Analysis of initial contact of milling cutter and work in relation to tool life. Trans. ASME **68**(3), 217 (1946)
10. Opitz, H., Beckhaus, H.: Influence of initial contact on tool life when face milling high strength materials. Ann. CIRP **18**(2), 96–103 (1970)
11. Jordberg, J.: Tool entry and exit in interrupted cutting. Royal Institute of Technology, KTH, Stockholm (1995)
12. Pekelharing, A.J.: Exit failure in interrupted cutting. Ann. CIRP **27**(1), 5–10 (1978)
13. Pekelharing, A.J.: Cutting tool damage in interrupted cutting. Wear **62**(1), 37–48 (1980)
14. Agic, A., Eynian, M., Hägglund, S., Ståhl, J.-E., Beno, T.: Influence of radial depth of cut on entry conditions and dynamics in face milling application. J. Superhard Mater. **39**(4), 259–270 (2017)
15. Sutherland, J.W.: A dynamic model of the cutting force system in the end milling process. Diss. Abstr. Int. **49**(1), 293 (1988)
16. Tobias, S.A., Fishwick, W.: The chatter of lathe tools under orthogonal cutting conditions. Trans. ASME **80**, 1079–1088 (1958)
17. Doi, S., Kato, S.: Chatter vibration of lathe tools. ASME Trans. **78**, 1127–1134 (1956)
18. Altintas, Y.: Analytical prediction of three dimensional chatter stability in milling. JSME Int J. Ser. C **44**(3), 717–723 (2001)
19. Brandt, A.: Noise and Vibration Analysis. Wiley, New York (2011)
20. Ståhl, J.E. Andersson, M., Zhou, J.M.: Load Analysis and Identification in Metal Cutting Process. LUTMDN/(TMMV-7024)/1-467/201. Lund University Lund (2001)
21. Tunç, L.T., Budak, E.: Effect of cutting conditions and tool geometry on process damping in machining. Int. J. Mach. Tools Manuf. **57**, 10–19 (2012)
22. Altintas, Y., Eynian, M., Onozuka, H.: Identification of dynamic cutting force coefficients and chatter stability with process damping. CIRP Ann. **57**(1), 371–374 (2008)
23. Ståhl J., AB, S.: Metal cutting: theories and models. Division of Production and Materials Engineering. Lund University in cooperation with Seco Tools (2012)
24. Choudhury, I.A., See, N.L., Zukhairi, M.: Machining with chamfered tools. J. Mater. Process. Technol. **170**(1–2), 115–120 (2005)
25. Fang, N., Wu, Q.: The effects of chamfered and honed tool edge geometry in machining of three aluminum alloys. Int. J. Mach. Tools Manuf. **45**(10), 1178–1187 (2005)
26. Ren, H., Altintas, Y.: Mechanics of machining with chamfered tools. J. Manuf. Sci. Eng. **122**(4), 650 (2000)